

This is an Accepted Manuscript of the article: Santos-Clotas, E., Cabrera-Codony, A., Comas, J., Martín, M.J. (2020). Biogas purification through membrane bioreactors: Experimental study on siloxane separation and biodegradation. *Separation and Purification Technology*, vol. 238, art. Núm. 116440. Available online at <https://doi.org/10.1016/j.seppur.2019.116440>

© 2020. This manuscript version is made available under the CC-BY-NC-ND 4.0 license <http://creativecommons.org/licenses/by-nc-nd/4.0/>



1 **Biogas purification through membrane bioreactors: experimental**
2 **study on siloxane separation and biodegradation**

3 Eric Santos-Clotas^a, Alba Cabrera-Codony^a, Joaquim Comas^{a,b}, Maria J. Martín^{a*}

4 ^aLEQUIA, Institute of the Environment. University of Girona, Campus Montilivi, Girona
5 17003, Catalonia, Spain

6 ^bICRA, Catalan Institute for Water Research, Girona, Spain.

7 *Corresponding author e-mail: maria.martin@udg.edu

8 **ABSTRACT**

9 Sewage biogas valorization to different energy applications is hampered by the presence of
10 volatile methyl siloxanes. Despite the high operating costs, adsorption onto activated carbon is
11 the most implemented technology for siloxane removal from biogas. In order to purify biogas
12 sustainably, the current work explores the diffusion of siloxanes (octamethylcyclotetrasiloxane
13 and decamethylcyclopentasiloxane) together with other biogas impurities (limonene, toluene and
14 hexane) through polydimethylsiloxane membranes. Abiotic tests revealed transport efficiencies
15 above 75% towards a clean air stream for most compounds, although the transport of the most
16 hydrophobic pollutants was challenged when water was circulated through the shell side of the
17 membrane. Moreover, the performance of a hollow-fiber membrane bioreactor, inoculated with
18 anaerobic active sludge, was evaluated towards biogas purification in anoxic conditions. Toluene
19 and limonene were successfully degraded, hexane's removal efficiency was positively correlated
20 with the residence time, and siloxanes removal was achieved up to 21%. CO₂ was detected in the
21 outlet gas as the mineralization product as well as some byproducts from the degradation of
22 limonene and siloxanes. The presence of 1% of O₂ in the gas, as a strategy to substitute the NO₃⁻
23 , efficiently supported high removal for volatile organic compounds and moderate for siloxanes,
24 which would ultimately reduce the operating costs of the technology.

26 **KEYWORDS**

27 Biogas purification; Membrane bioreactor; Siloxanes; Volatile Organic Compounds

28 **1. INTRODUCTION**

29 Biogas production arises from the anaerobic digestion of the enormous quantities of sludge
30 generated in wastewater treatment plants (WWTP) and also in landfills. Biogas exploitation is
31 currently increasing owing to its energy applications given by the high methane content, while
32 restricting the release of greenhouse gases (GHG) into the atmosphere. Besides the major
33 compounds constituting biogas mixtures (i.e. CH₄ and CO₂), there is a large variability of
34 impurities, including alkanes, aromatic hydrocarbons and halogens (Bak *et al.*, 2019; Papadias *et*
35 *al.*, 2011). Hydrogen sulfide (H₂S) is one of the impurities found at higher concentrations, ranging
36 from 1000 to 20000 ppm_v and has damaging corrosive properties to the combustion engines
37 (Montebello *et al.*, 2014). Thus, it must be removed or reduced to different levels depending on
38 the use of biogas (Papurello *et al.*, 2019; Santos-Clotas *et al.*, 2019b).

39 On the other hand, volatile organic silicon compounds (i.e. siloxanes) have been found to be the
40 most harmful pollutants in energy recovery systems (ERS) during biogas valorization due to the
41 abrasive character of SiO₂, which is the conversion product of siloxanes after biogas combustion
42 (Soreanu *et al.*, 2011). Their occurrence in sewage biogas arises from their presence in cosmetics,
43 personal care products, shampoos, detergents and many more everyday products that eventually
44 reach the WWTPs (Zhang *et al.*, 2011). Given their low solubility in water and their liposoluble
45 nature, siloxanes are adsorbed onto the sludge flocs that reach the anaerobic digester where they
46 are volatilized with biogas due to the elevated temperatures (Dewil *et al.*, 2006).

47 To meet the energy demand in the treatment facility, biogas can be converted into heat and energy
48 by microturbines and internal combustion engines (ICE). Depending on the final biogas
49 conversion system, upgrading steps will be imperative according to the manufacturer's
50 requirements. In this sense, siloxane concentration in biogas prior to its valorization in
51 microturbines or fuel cells must be decreased to levels below 0.03 or 0.1 mg m⁻³, respectively (de
52 Arespachoga *et al.*, 2015; Santos-Clotas *et al.*, 2019b). Biogas can also be injected into the

53 domestic gas grids or it can be used as a car fuel after undergoing upgrading measures to fulfill
54 the legislative demands which is regulated by the country-dependent national laws. For instance,
55 siloxane concentration in biogas must be below 10 mg m⁻³ in Spain and Austria, or below 6 mg
56 m⁻³ in Czech Republic prior to its injection into the national gas grids (Muñoz *et al.*, 2015).

57 Conventional technologies used for siloxane abatement are based on non-regenerative adsorption
58 onto fixed beds of activated carbon (AC) (Cabrera-Codony *et al.*, 2015). Steam ACs are
59 frequently used in such application even though scientific reports highlight a superior siloxane
60 adsorption capacity by chemically activated carbons (Cabrera-Codony *et al.*, 2018, 2014). Other
61 physical/chemical technologies for siloxane abatement include absorption into strong acids and
62 bases such as H₂SO₄, HNO₃ and NaOH (Schweigkofler and Niessner, 2001), and deep chilling in
63 which siloxanes are condensed by reducing the temperature of biogas to 5°C or even below -20°C
64 (Wheless and Pierce, 2004). Biological technologies for siloxane removal from biogas are under
65 investigation at lab-scale including biotrickling filtration (BTF) and membrane bioreactors
66 (MBR) among others.

67 Biotrickling filtration has resulted as an efficient technique in handling odor-laden gases as well
68 as biogas desulfurization (Lebrero *et al.*, 2012; Montebello *et al.*, 2014). Some scientific papers
69 are found in the literature reporting on the biological elimination of siloxanes in biotrickling filters
70 identifying mass transfer as the main limitation for siloxane elimination (Accettola *et al.*, 2008;
71 Popat and Deshusses, 2008). Most of the studies in the literature assessing siloxane removal from
72 biogas with biotechnologies are conducted in aerobic conditions (i.e. O₂ as the final electron
73 acceptor) by providing air as the synthetic gas matrix. Since oxygen composition in biogas is
74 generally found below 1%, and more importantly due to explosion risks it is crucial to investigate
75 siloxane removal using other electron acceptors. In this sense, Santos-Clotas *et al.*, (2019a)
76 studied the removal of octamethylcyclotetrasiloxane (D4) and decamethylcyclopentasiloxane
77 (D5) in an anoxic BTF by supplying NO₃⁻ in the trickling solution. D5 (37%) removal was higher
78 than D4 (13%), especially when the packing bed of the BTF was supplemented with activated
79 carbon which boosted D5's removal efficiency up to 45%. In this regard, siloxane degradation

80 studies with different isolates from anaerobic batch enrichment cultures proved that D5 was more
81 biodegradable than D4 (Boada *et al.*, 2020).

82 On the other hand, membrane bioreactors (MBR) are based on the transference of gas pollutants
83 from one side of the membrane to the other, where a biofilm is developed over the surface of the
84 membrane and is in contact with a nutrient-containing mineral medium. Several types of
85 membranes are found commercially. Dense membranes are more selective, but their ability to
86 diffuse the pollutants through the fibers depends on the contaminant's solubility and diffusivity
87 (Kumar *et al.*, 2008b). The driving force for the pollutants to permeate through the membrane
88 relies on the concentration gradient between both sides, thus depending on the ability of the
89 microbial population to degrade the contaminants (Reij *et al.*, 1998). Membranes are capable of
90 selectively permeate pollutants that are hardly transferred using other reactor configurations
91 (Barbusinski *et al.*, 2017). Few scientific reports assess the treatment of gas streams containing
92 volatile organic compounds (VOC), such as toluene, benzene and hexane among others, in lab or
93 pilot scale MBRs (Kumar *et al.*, 2008a; Lebrero *et al.*, 2014) as well as H₂S in biogas (Pokorna-
94 Krayzelova *et al.*, 2017). Considering biogas treatment, siloxane permeation through
95 polydimethylsiloxane (PDMS) membranes was only evaluated with clean air flowing in the other
96 side of the membrane, who reported high removal efficiencies for both cyclic and linear siloxanes
97 (Ajhar *et al.*, 2012). However, no reports are found on biogas purification by means of MBRs.

98 The aim of this study is to investigate the performance of a hollow-fiber membrane bioreactor
99 inoculated with anaerobic digester sludge on the removal of siloxanes and other occurrent volatile
100 organic compounds in biogas. The abiotic transference through a PDMS membrane towards clean
101 air and water will be assessed as well as different strategies related to the final electron acceptor
102 will be evaluated in order to optimize the bioreactor.

103

104 2. MATERIALS AND METHODS

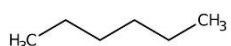
105 2.1 Synthetic biogas

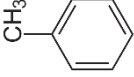
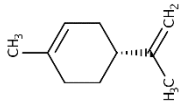
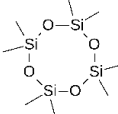
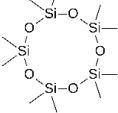
106 The synthetic biogas used for conducting this research consisted in nitrogen as the gas matrix
107 spiked with three VOC (hexane, toluene and limonene) and two siloxanes
108 (octamethylcyclotetrasiloxane D4, and decamethylcyclopentasiloxane D5) based on their
109 common occurrence in anaerobic digester biogas (Papadias *et al.*, 2011).

110 Liquid reagents of D4 (98%), D5 (97%), toluene (99.8%), D-limonene (97%) and n-hexane (99%)
111 (Sigma Aldrich) were used for the present work. The liquid reagent of each target compound was
112 added to a septum-sealed vial and weighted in an analytical balance (XSR105 Mettler Toledo,
113 USA). The vial was shaken at 200 rpm in an orbital shaker (3005, GFL) for 30 minutes to
114 guarantee homogeneity. The resulting mixture was accurately injected at 18 $\mu\text{L h}^{-1}$ by a syringe
115 pump (11 Elite, Harvard Apparatus) through a septum in a tee union (Swagelok, USA) to a N_2
116 stream (99.999%, Abelló Linde, Spain) regulated by a mass flow controller (MC Series, Alicat
117 Scientific). The synthetic gas generated was homogenized in four static mixers (Koflo, Cole
118 Parmer, USA) connected in series followed by a mixing chamber. The target concentrations (C_0)
119 as well as main physical and chemical properties of the target pollutants are detailed in Table 1.

120 The inlet and outlet gas composition were analyzed by a flow-through gas sampling valve in a
121 gas chromatograph equipped with a flame ionization detector (GC-FID, 7890B Agilent
122 Technologies). Separation of the target pollutants was carried out by a HP-5ms Ultra Inert
123 capillary column (Agilent Technologies). Standards for calibration purposes were obtained by
124 injecting the target mixture (Table 1) to different N_2 flows. Detection limit for siloxanes was 1
125 mg m^{-3} while for VOCs was 0.5 mg m^{-3} . Analysis of the inlet and outlet gas streams was performed
126 in triplicate (coefficient of variation < 5%).

Table 1. Main properties and feed gas concentration of the target compounds

Compound	Formula	MW [g mol ⁻¹]	Water solubility [mg L ⁻¹]	C_0 [mg m ⁻³]	Henry's constant [atm m ³ mol ⁻¹]
Hexane		86.2	9.5	375 ± 18	1.80

Toluene		92.1	526	24 ± 2	6.64×10^{-3}
Limonene		136.2	13.8	220 ± 11	2.81×10^{-2}
D4		296.6	0.056	54 ± 3	12.00
D5		370.7	0.017	102 ± 4	33.00

*in water at 25 °C according to PubChem library

127

128 2.2 Gas abiotic experiments

129 The PDMS membrane module employed for the first set of gas abiotic experiments was the
 130 PermSelect PDMSXA-10 (MedArray Inc, USA), consisting of 30 parallel dense hollow fibers of
 131 190 μm inner diameter and 300 μm outer diameter. The membrane area was estimated at 10 cm^2
 132 and a lumen-side priming volume of 0.67 cm^3 . The test gas was flown through the lumen side
 133 (inside fibers) at 50 mL min^{-1} leading to a gas residence time (GRT) of 0.72 s. On the other side
 134 of the fibers, i.e. the shell side, a clean N_2 stream was provided as displayed in Fig. 1 at rates
 135 ranging from 25 to 400 mL min^{-1} , leading to different shell-to-lumen flow ratios (0.5, 1, 2, 4 and
 136 8).

137 For each experiment, the test gas run overnight to reach steady state, due to the certain adsorption
 138 of the compounds in the membrane fibers taking place during the first operation hours.

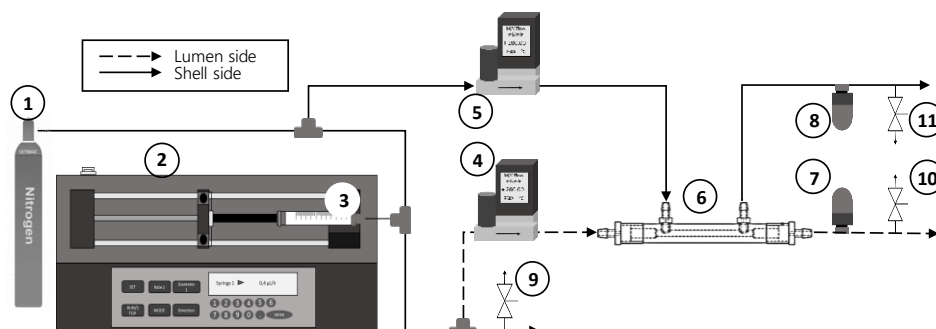


Fig. 1. Membrane setup for gas abiotic experiments: (1) N_2 cylinder; (2) Syringe pump; (3) 250-mL syringe with mixture; (4, 5) Mass flow controllers; (6) Hollow-fiber membrane (PDMSXA-10); (7, 8) Pressure transducers and (9, 10, 11) sampling ports for GC analysis.

139

140 2.3 Hollow-fiber membrane bioreactor (HF-MBR)

141 The reactor used was a commercial hollow-fiber module (PDMSXA-2500, PermSelect®,
142 MedArrays Inc, USA) that consisted of 3200 hollow fibers of 190 and 300 μm inner and outer
143 diameter, respectively. The total membrane area accounted for 2500 cm^2 and a lumen-side
144 priming volume of 21 cm^3 . The synthetic test gas with the compounds in Table 1 was generated
145 as described previously (section 2.1) and humidified through a gas wash bottle. The inlet gas was
146 regulated by a mass flow controller and fed through the lumen side of the membrane module. Fig.
147 2 shows a schematic representation of the lab-scale hollow-fiber membrane bioreactor setup.

148 Through the shell side, the synthetic mineral medium with nutrients was recycled at 50 rpm (100
149 mL min^{-1}) by a peristaltic pump (323S Watson Marlow, USA) from an external reservoir
150 continuously agitated.

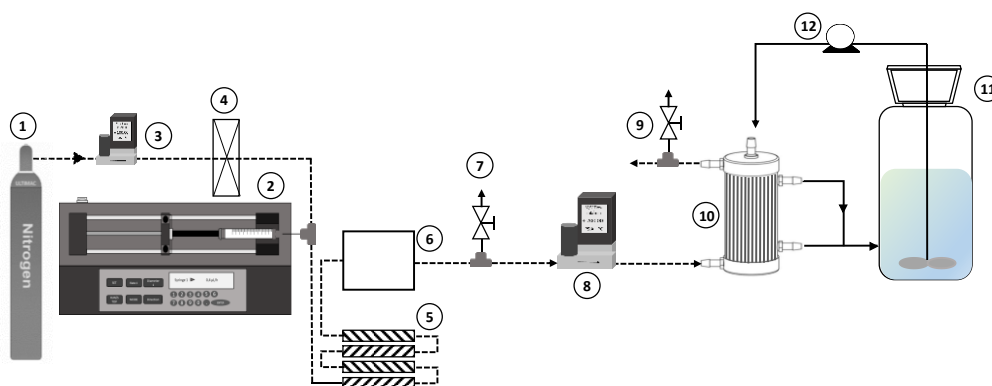


Fig. 2. Schematic representation of the HF-MBR. 1 N_2 bottle; 2 Syringe pump; 3 and 8 Mass flow controllers; 4 Water column; 5 Static mixers; 6 Mixing chamber; 7 and 9 Sampling points; 10 HF-MBR; 11 Nutrients reservoir; 12 Peristaltic pump

151

152 2.3.1 Abiotic operation

153 In a close-loop system where water is continuously recirculated, the pollutants' mass transfer
154 depends on their solubility besides the transport efficiency of the membrane. So once the water
155 had absorbed the maximum concentration possible for each compound, their mass transfer tends
156 to zero. In order to approach a bioreactor configuration, in which a liquid media is found in one
157 side of the membrane, the capacity of the contaminants to permeate from the lumen side towards
158 water in the shell side was investigated. An open-loop configuration with clean water

159 continuously circulating through the membrane (water/gas) was set-up before inoculating the HF-
160 MBR. The abiotic mass transfer characterization of the target VOCs and siloxanes was conducted
161 according to Lebrero *et al.*, (2014) at different GRTs. The test gas was supplied through the lumen
162 side whereas a clean water flow was circulated at a constant flow of 100 mL min⁻¹ through the
163 shell side of the module. The abiotic transfer of the target pollutants was evaluated at 9.6, 16, 24,
164 40 and 60 s of GRT by monitoring their concentration in the inlet and outlet of the lumen and
165 calculating the transport efficiency (in %) as in Eq. 1.

166 2.3.2 *Inoculum and synthetic mineral medium*

167 Anaerobic sludge from the anaerobic digester of the urban wastewater treatment plant of Girona
168 (Spain) was used as inoculum in the membrane bioreactor. In order to remove the dissolved
169 organic matter from the sludge, the following procedure was carried out 3 times: centrifugation
170 at 10000 rpm for 10 min (EBA 21, Hettich), pouring the remaining water and re-suspension with
171 fresh mineral medium. The sludge was diluted to a final concentration of 4.2 g TSS L⁻¹, and 250
172 mL of the cleaned and diluted sludge were used as MBR inoculum.

173 The synthetic mineral medium was composed of (in g L⁻¹): 1 NaCl; 0.2 MgSO₄·7H₂O; 0.02
174 CaCl₂·2H₂O; 0.04 NH₄Cl; 1.16 KH₂PO₄·H₂O; 4.76 of HEPES buffering agent. The pH was
175 adjusted to 6.9 using NaOH 1 M. The resulting mineral medium was used for both the sludge
176 resuspension previously described and the recycling solution in the MBR operation. Anoxic
177 conditions were provided with 2 g L⁻¹ of NaNO₃⁻ in the mineral medium.

178 2.3.3 *Operating conditions*

179 The membrane module was inoculated with 250 mL of the cleaned sludge corresponding to a
180 concentration of 4.2 g TSS L⁻¹ and operated at different conditions as summarized in Table 2.
181 During stage I, 1-36 days, the GRT was 18 s, corresponding to a gas flow of 70 mL min⁻¹. The
182 recirculating solution was renewed every 72 hours corresponding to a dilution rate of 0.3 d⁻¹. The
183 influence of the GRT on the removal of the target pollutants was evaluated by increasing it to
184 31.5 s (period II days 37-64) and 63 s (days 65-73).

185 Automatic NO_3^- supply system started at day 73 by injecting a solution of $200 \text{ g NO}_3^- \text{ L}^{-1}$
 186 (provided by NaNO_3 of 99% purity) to the recirculation solution by means of a syringe pump (11
 187 Elite, Harvard Apparatus) adjusted to maintain a stable concentration over 2.5 g L^{-1} , and the
 188 dilution rate of the recirculation solution was decreased to 0.1 d^{-1} .

189 In the stage IV-a (days 101-133), the GRT was decreased back to 18 s for comparison reasons. A
 190 membrane cleaning was carried out at day 107 following the procedure described by Lebrero *et*
 191 *al.*, (2014), which consisted in increasing the liquid recycling rate in order to slough off the
 192 biomass clogging.

193 In stage IV-b the carrier gas was supplemented with 1% of O_2 at day 134, based on the common
 194 O_2 content in biogas (Rasi *et al.*, 2007), and was operated with NO_3^- and O_2 as final electron
 195 acceptors until day 152. Finally, from day 153 to 164 (stage IV-c), the reactor was operated with
 196 only O_2 and the automatic infusion of NO_3^- was stopped.

Table 2. Operating conditions of the HF-MBR.

Stage	Period [days]	GRT [s]	Final e ⁻ acceptor	NO_3^- supply
I	1-36	18	NO_3^-	Manual
II	37-64	31.5	NO_3^-	Manual
III	-a	65-73	NO_3^-	Manual
	-b	74-100	NO_3^-	Automatic
IV	-a	101-133	NO_3^-	Automatic
	-b	134-152	$\text{NO}_3^- + \text{O}_2$	Automatic
	-c	153-164	O_2	Automatic

197 2.3.4 Analytical procedures

198 NO_3^- concentration in the recycling solution of the HF-MBR was analyzed by a
 199 Spectrophotometer (Cary3500, Agilent Technologies) following the Standard Methods 4500-
 200 NO_3^- (APHA, 1998). Identification of biodegradation by-products in the trickling solution was
 201 conducted by means of a Gas Chromatography coupled to a Mass Spectrometry detector (GC-
 202 MS, 7890B-5977B, Agilent Technologies) as described in (Santos-Clotas *et al.*, 2019a) and α - ω -
 203 silanediols determination was carried out following the procedure reported by Cabrera-Codony
 204 *et al.*, (2017). Pure commercial reagents were injected in the GC-MS for further confirmation.

205 CO₂ in the effluent of the HF-MBR (lumen side) was analyzed by means of a gas sampling valve
206 in the GC-MS described above, by monitoring the ion with m/z 44. Calibration standards were
207 prepared by diluting CO₂ (99.99%, Abelló Linde, Spain) to different N₂ streams.

208 The performance of the HF-MBR was evaluated by the removal efficiency (RE) and the
209 elimination capacity (EC) following Eq. 1 and Eq. 2, respectively, considering the analysis of the
210 inlet and outlet streams flowing through the lumen side of the membrane. In order to evaluate the
211 biological degradation, the carbon mineralization efficiency (CME) was defined as in Eq. 3.

$$RE (\%) = \left(\frac{C_0 - C_F}{C_0} \right) \times 100 \quad \text{Eq. 1}$$

$$EC (g m^{-3} h^{-1}) = \left(\frac{(C_0 - C_F) \times Q}{V} \right) \quad \text{Eq. 2}$$

$$CME (\%) = \left(\frac{P_{CO_2}}{\sum_i EC_i} \right) \times 100 \quad \text{Eq. 3}$$

212 Where C₀ and C_F are the target compound concentrations (g m⁻³) in the inlet and outlet of the HF-
213 MBR, Q is the gas flow (m³ h⁻¹) and V the reactor volume (m³). In Eq. 3 P_{CO₂} refers to the C
214 produced as CO₂ detected in the lumen outlet (g C m⁻³ h⁻¹), *i* refers to each target pollutant (i.e.
215 hexane, toluene, etc.) and EC the elimination capacity expressed as g C m⁻³ h⁻¹ of each pollutant.

216 **3. RESULTS AND DISCUSSION**

217 **3.1 Abiotic diffusion of the pollutants**

218 *3.1.1 Towards clean air*

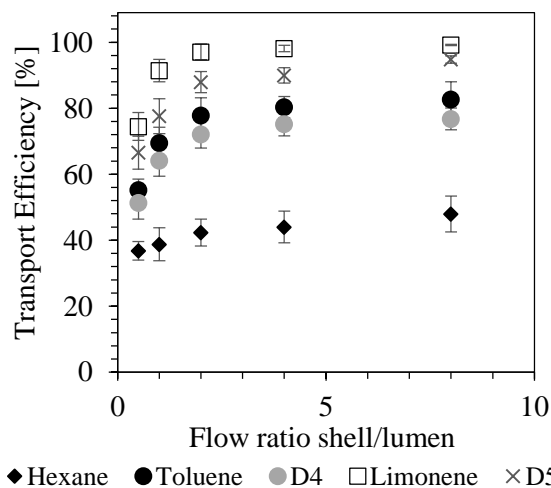
219 The capacity of the PDMS membrane module to separate the target pollutants was investigated
220 in gas abiotic experiments. Each target compound concentration was monitored in the feed gas
221 and in both the lumen and the shell outlet streams. Experiments were done by triplicate with a
222 relative error below 5%.

223 The transport efficiency of most compounds, reported in Fig.3, displayed a clear steep increase
224 with the shell/lumen flow ratio. Incrementing the flow of clean gas in the shell side distinctly
225 boosted the transference of the target pollutants through the membrane. In the case of limonene

226 and D5, their transport increased from 66.5 and 74.5% at the lowest ratio, respectively, up to 94.8
227 and 99.2 at the highest ratio 8. The transport of toluene and D4 went respectively from 55.2 and
228 51.4% up to 82.7 and 76.8% by increasing the shell/lumen ratio from 0.5 to 8. Contrarily, hexane
229 was the compound with the lowest transport efficiencies, demonstrating a moderate increase from
230 36.8 to 48% from 0.5 to 8 ratios.

231 The transport efficiency of all pollutants, excluding hexane, through the membrane was above
232 50% even at the lowest shell/lumen ratio tested, demonstrating that operating at such a short
233 residence time (i.e. 0.72 s), and with a low gas flow through the shell side, the target pollutants
234 were successfully permeated through the membrane. These results point out that the PDMS
235 membrane had a high selectivity towards the target compounds, except for hexane. Moreover, as
236 a result of incrementing the shell flow, the transport efficiencies increased, which indicated that
237 the driving force for the compounds to permeate through the membrane was incremented as well.
238 Moreover, the diffusion of all compounds levelled off at a flow ratio of 2, where high transport
239 efficiencies were already recorded, being 97.1, 87.9, 77.8 and 72.1% for limonene, D5, toluene
240 and D4, respectively. Therefore, incrementing the shell flow from 100 up to 400 mL min⁻¹ (i.e.
241 shell/lumen flow ratio from 2 to 8) did not significantly improve the pollutants transport.

242 Similar experiments were carried out by Ajhar *et al.*, (2012) using the same membrane module
243 with gas spiked with cyclic and linear siloxanes, and high permeabilities for the siloxane D4 and
244 D5 were reported. Their siloxane removal, for both D4 and D5, appeared above 70% when the
245 flow ratio was higher than 2, and also D5 removal was slightly higher than D4. Siloxane transport
246 in the present study were obtained slightly higher despite the presence of VOCs.



◆ Hexane ● Toluene ● D4 □ Limonene × D5
 Fig. 3. Transport efficiency through the membrane in gas/gas experiments at different shell/lumen flow ratios.

247

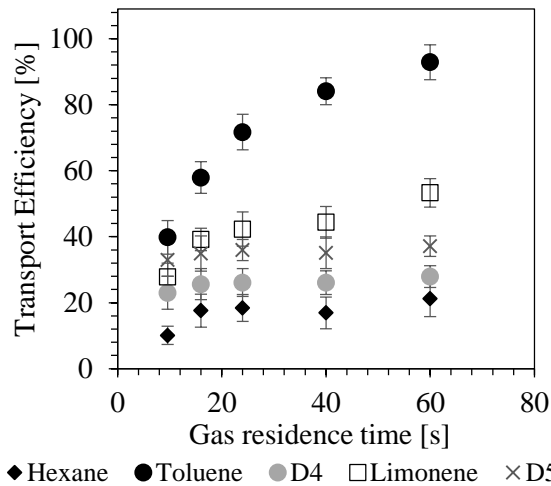
248 *3.1.2 Towards clean water*

249 The transport efficiency of each compound was evaluated at different GRTs as function of the
 250 test gas flow through the lumen side: 9.6, 16, 24, 40 and 60 s. Results for each compound are
 251 shown in Fig. 4.

252 A noticeable linear increase in the transport efficiency with the residence time was observed for
 253 toluene, which was the compound with the highest water solubility. At 9.6 s its transport across
 254 the membrane was of 40% and it raised up to 84 and 93% when the GRT was increased to 40 and
 255 60 s, respectively. The transport efficiency of limonene increased from 28% at 9.6 s up to 53% at
 256 60 s, although the improvement from 16 (39%) to 40 s (44%) was not significant, which might
 257 be explained by the relatively low solubility of limonene in water. For the same reason, D4, D5
 258 and hexane, that are low water-soluble compounds, were less transported through the membrane
 259 than toluene and limonene. Maximum transport efficiencies for D4, D5 and hexane were 28, 37
 260 and 21%, respectively, obtained at 60 s of residence time.

261 The PDMS membrane was capable of permeating both siloxanes in the abiotic gas experiments,
 262 but when water was present in the other side of the membrane, their diffusion was hampered due
 263 to their low solubility. In the case of hexane, a lower affinity with the membrane material than for
 264 the rest of pollutants was observed in the abiotic gas experiments, and the presence of a liquid

265 media did not improve its permeation through the membrane, which is in good agreement with
266 Lebrero *et al.*, (2014). In this sense, even with much higher residence time in comparison with
267 the gas experiments, the transfer of the compounds was limited to their Henry's law coefficients.



◆ Hexane ● Toluene ● D4 □ Limonene × D5
Fig. 4. Transport efficiency through the membrane in water/gas tests at different GRTs.

268

269 3.2 HF-MBR performance

270 3.2.1 Start-up of the HF-MBR

271 The HF-MBR was inoculated with anaerobic sludge from an urban WWTP and fed with the
272 synthetic gas stream as in the abiotic experiments, detailed in Table 1. The outlet of the membrane
273 was continuously monitored for evaluating the RE and EC of each target compound and the whole
274 set of data obtained is plotted in Fig. 5 for each operation period as described in Table 2.

275 The reactor was initially run at a GRT of 18 s (stage I, days 0-36), corresponding to the first period
276 of operation where the NO_3^- provided by the synthetic mineral media in the shell side of the HF-
277 MBR was used by the biofilm as final electron acceptor. In this acclimation period the removal
278 of both siloxanes was highly fluctuant, around $1 \text{ g m}^{-3} \text{ h}^{-1}$ of D4 and $3 \text{ g m}^{-3} \text{ h}^{-1}$ of D5. These
279 elimination capacities correspond to removal efficiencies from 4 to 14% for D4 (Fig. 5D) and
280 from 2 to 23% in the case of D5 (Fig. 5E).

281 On the other hand, steady state for toluene and limonene (Fig. 5B and C) biodegradation was
282 achieved within 7-8 days reaching average REs of 52 ± 2 and $85 \pm 3\%$, respectively, which

283 corresponded to ECs of 2.4 ± 0.1 and 33.5 ± 1.2 g m⁻³ h⁻¹. In the abiotic experiments with a clean
284 water stream circulating continuously, the transport efficiency of these target VOCs at 16 s of
285 GRT was 39.2% and 57.9% for limonene and toluene respectively. Therefore, the presence of a
286 biofilm in the shell side of the membrane clearly promoted a higher elimination of these target
287 VOCs. The degradation of these compounds favored their diffusion through the membrane, which
288 led to higher REs.

289 Regarding hexane removal, steady state was achieved after 15 days with an average EC of 2.1 g
290 m⁻³ h⁻¹ (corresponding to a RE of 4%, Fig. 5A). Indeed, hexane abatement was expected to be
291 lower than the other VOCs due to the low diffusion through the membrane previously observed
292 in the abiotic experiments. Hexane's transference through the PDMS membrane was also
293 hampered by a low mass transfer to the aqueous media, which would be in agreement with
294 Lebrero *et al.*, (2014). However, Zhao *et al.*, (2011) reported that hexane biodegradation was
295 inhibited by the presence of toluene during the co-treatment of hexane and toluene mixtures in a
296 HF-MBR. In this sense, an inhibition effect could not be ruled out although the inlet
297 concentrations in the present study were much lower than in the aforementioned study.

298

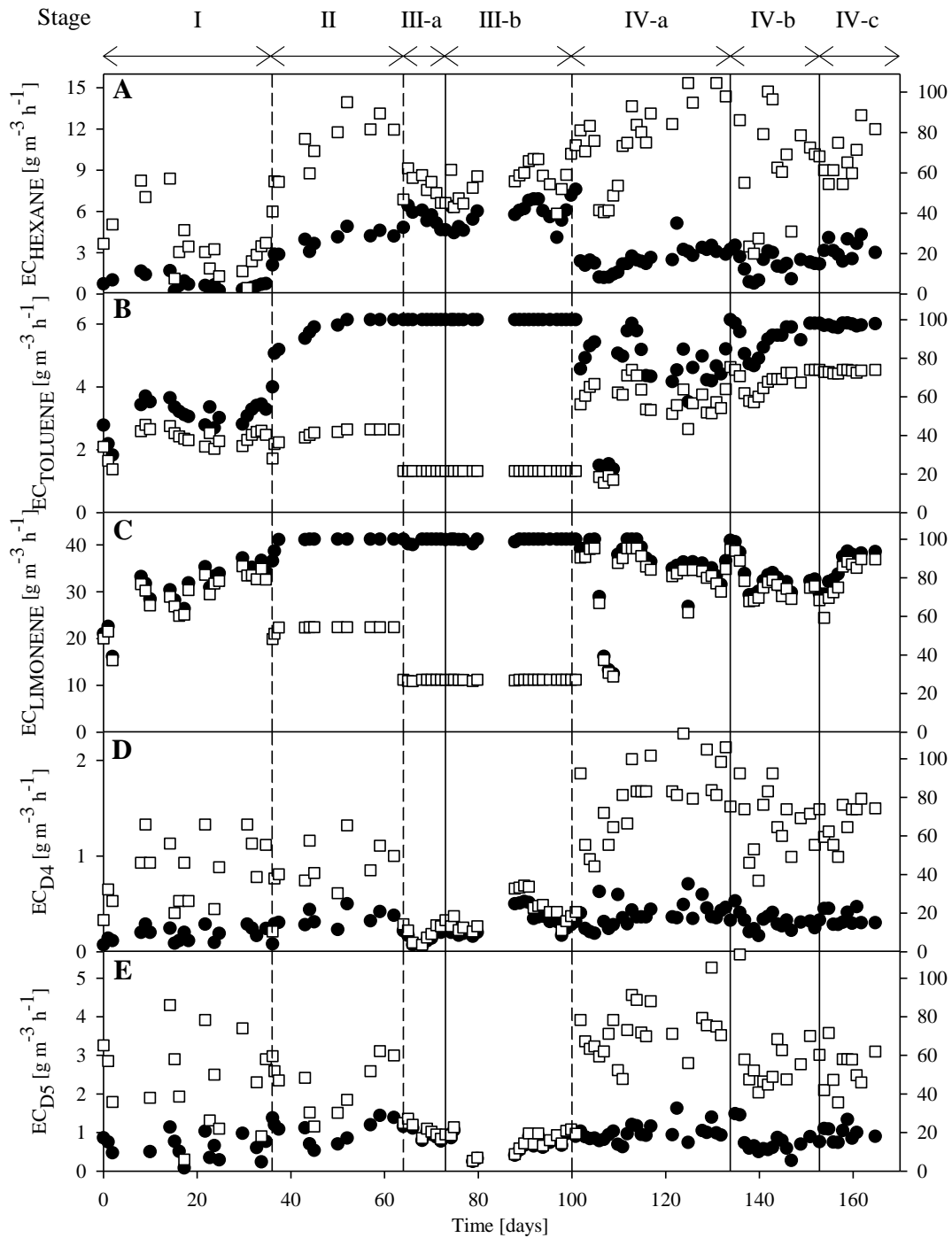


Fig. 5. Time-course of the removal efficiency (RE, ●) and elimination capacity (EC, □) of hexane (A), toluene (B), limonene (C), D4 (D) and D5 (E). Dashed lines indicate changes in the GRT (31.5, 63 and 18 s). Solid lines represent the strategies set for the electron acceptor (Automatic NO_3^- injection, 1% O_2 supply and NO_3^- injection stoppage).

299

300 *3.2.2 Influence of the gas residence time*

301 In order to improve the abatement of the target compounds, the GRT was increased to 31.5 s in

302 the second stage (stage II, days 37-64). In this scenario, the removal of siloxanes increased up to

303 REs 17 ± 6 and $21 \pm 6\%$ for D4 and D5, respectively, where the ECs accounted for average values
304 of 1.0 ± 0.2 and $2.5 \pm 0.7 \text{ g m}^{-3} \text{ h}^{-1}$. The stability of the siloxanes' removal continued displaying
305 ups and downs along the time-course of the reactor operation in spite of the higher GRT provided.
306 The lack of significant correlation between siloxane removal efficiency and the GRT, indicates
307 that their diffusion through the membrane towards the liquid side was limited due to their
308 hydrophobicity regardless the residence time. Even though an increased RE was obtained for both
309 siloxanes from 18 to 31.5 s, no further improvement was achieved at 60 s of GRT. To the authors'
310 knowledge, this is the first study operating an MBR towards the removal of siloxanes from biogas.
311 However, some reports in the literature investigated the biodegradation of cyclic siloxanes in
312 BTFs and agreed that mass transfer limitations hamper siloxane biodegradation (Accettola *et al.*,
313 2008; Popat and Deshusses, 2008). More recently, the performance of an anoxic BTF towards a
314 VOC-siloxane mixture was investigated and REs of 20 and 37% for D4 and D5, respectively,
315 were reported (Santos-Clotas *et al.*, 2019a).

316 It is important to stress that the use of MBR ultimately entails lower reactor sizes than those
317 necessary in BTF performing similarly, since the gas residence time in the BTF was 14 min, well
318 above the GRT studied in the present HF-MBR (18-60 s).

319 Contrarily, the longer residence time led to a rapid increase in the RE of all the VOCs (Fig. 5A,
320 B and C). Hexane reached a steady state RE of $30 \pm 6\%$ corresponding to an EC of $12.5 \pm 1.2 \text{ g}$
321 $\text{m}^{-3} \text{ h}^{-1}$. Toluene gradually increased until its absence in the outlet gas stream (i.e. below the
322 detection limit of the analytical method) at day 52, which indicated that it was completely
323 transferred through the membrane achieving an EC up to $2.6 \pm 0.3 \text{ g m}^{-3} \text{ h}^{-1}$. Several scientific
324 papers agree on the efficiency of MBRs for the removal of this aromatic hydrocarbon reporting
325 elimination capacities up to $1500 \text{ g m}^{-3} \text{ h}^{-1}$ at GRTs in the range 0.9-60 s (Mudliar *et al.*, 2010).
326 Most toluene ECs reported are much higher than in the present work given the low flows treated
327 as well as the low concentration in biogas. Limonene displayed a similar but even faster trend
328 since, just right the day after increasing the residence time, its removal was already complete

329 reaching an EC of $22.4 \text{ g m}^{-3} \text{ h}^{-1}$. REs as high as 98% for limonene were obtained in a flat-sheet
330 MBR treating a mixture of VOCs at a GRT of 30 s (Lebrero *et al.*, 2013).

331 The GRT was further increased to 63 s in the third period (stage III, days 65-100). Toluene and
332 limonene REs remained at 100%, as expected. while the RE of hexane increased up to $43 \pm 7\%$,
333 much higher than the diffusion recorded in the water abiotic tests. Average ECs within this were
334 1.3 , 11.2 and $8.2 \text{ g m}^{-3} \text{ h}^{-1}$ for toluene, limonene and hexane, respectively. The abatement of
335 siloxanes slightly decreased to $14 \pm 4\%$ for D4 and $17 \pm 2\%$ for D5.

336 Overall, toluene and limonene were completely removed when the HF-MBR was operated at
337 GRTs longer than 18 s, although even at such short contact time removals were found above 80%
338 for both pollutants. As regarded in Fig. 6 the RE of these VOCs was positively influenced by
339 increasing the gas residence time. The removal of hexane also appeared to be boosted with higher
340 residence times from 17% at 18 s up to an average RE of 42% at 63 s.

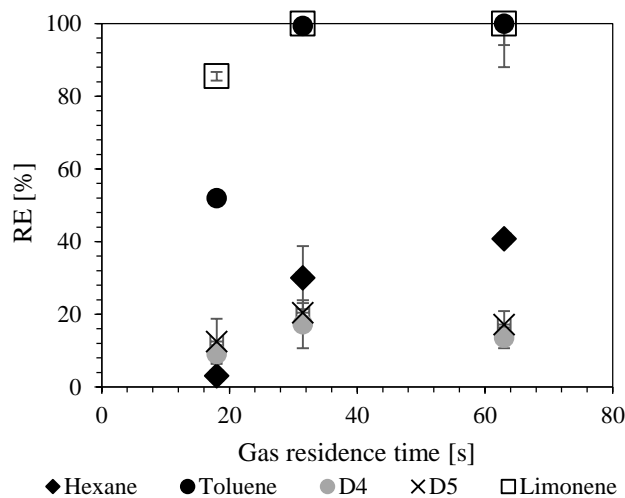


Fig. 6. Influence of the gas residence time on the RE of the target compounds at steady state of the HF-MBR (Stages I,II,III-a).

341

342 3.2.3 Fate of biodegradation products

343 In order to study the fate of the biodegradation products, the outlet gas was analyzed by GC-MS.
344 Carbon mineralization efficiency was determined by the CO_2 formation, as final product of target
345 compounds mineralization. Thus, Fig. 7A depicts the carbon removed as the sum of target
346 compounds and the carbon formed in CO_2 form in the lumen side of the membrane. It is important

347 to highlight that an irregular gas emission was detected through the shell side from the nutrient
348 reservoir. GC-MS analysis revealed the presence of CO₂ in such emission, indicating that a minor
349 contribution of the CO₂ released from the pollutants' biodegradation did not permeate through the
350 membrane. Due to the scarce flow (below 4 mL min⁻¹) and its intermittence, this shell-side
351 emission was not monitored neither accounted for in the CME calculations. Thus, most of the
352 formed CO₂ was found in the lumen emission, given its capacity to permeate through the
353 membrane, as reported by Ajhar *et al.*,P (2012), and the gas driving force in the lumen side.

354 The CME within Stage II was roughly 60%, suggesting a partial oxidation of the target
355 compounds and the subsequent accumulation of biodegradation byproducts. In this context, the
356 presence of a byproduct was recorded in the outlet emission of the reactor, which was later
357 identified as α -terpinene by means of GC-MS analysis and a match higher than 90% with NIST
358 library. The occurrence of such byproduct was related to an incomplete oxidation of limonene, as
359 suggested by Santos-Clotas *et al.*, (2019a) in an anoxic BTF when the input of NO₃⁻ in the
360 trickling solution was limited due to interruptions on the irrigation system.

361 Furthermore, GC-MS analysis of the recirculation solution revealed the presence of
362 dimethylsilanediol, which could not be quantified due to the lack of pure commercial standards,
363 but has been described as one of the main metabolites of cyclic siloxanes biodegradation (Wang
364 *et al.*, 2014).

365 In Stage III, the beneficial role of a higher GRT (i.e. 63 s) was noticed with a complete removal
366 of both toluene and limonene (Fig. 5B and 5C, respectively). Moreover, the presence of α -
367 terpinene was no longer recorded, suggesting that limonene was completely degraded. This was
368 confirmed with a CME as high as 91 ± 6 %, where the carbon produced in CO₂ form detected in
369 the lumen emission almost matched the carbon removed from the target compounds degradation
370 (Fig. 7A).

371

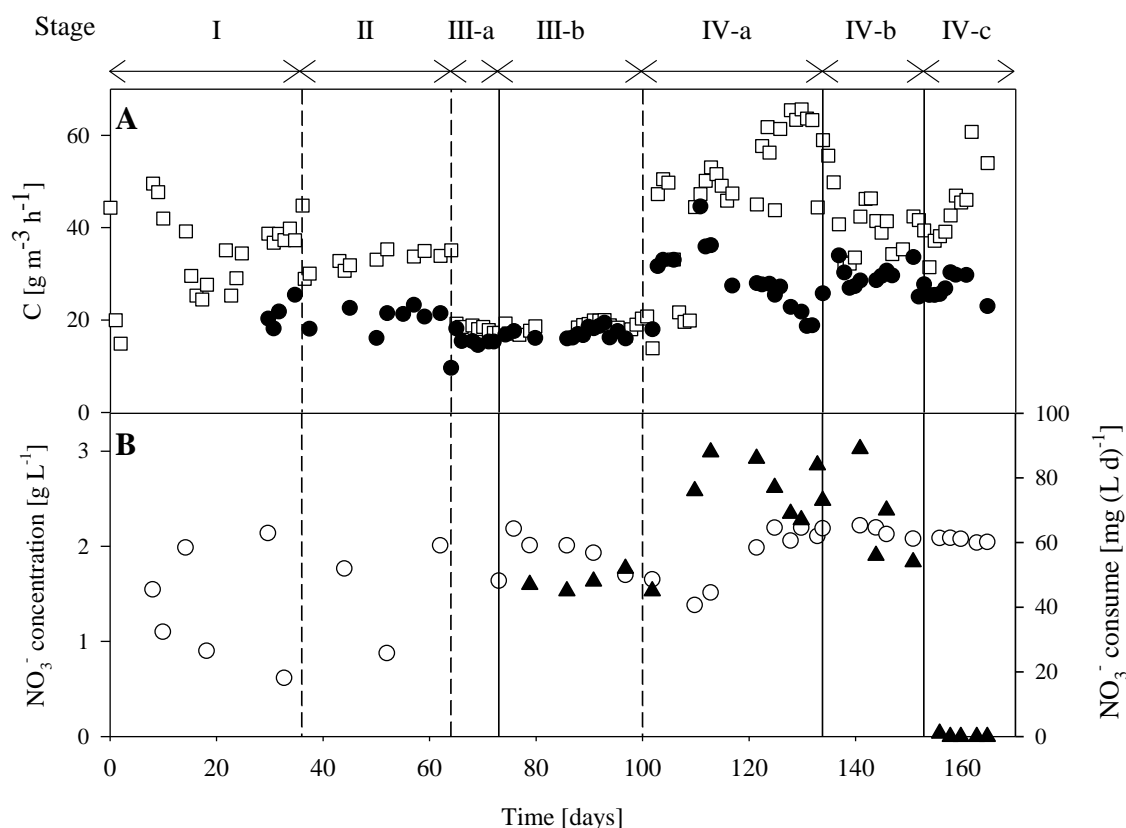


Fig. 7. Time-course of (A) carbon removed from target compounds degradation (\square) and carbon produced in CO_2 form (\bullet); and (B) the NO_3^- concentration in the recirculation mineral medium (\circ) and NO_3^- consume (\blacktriangle). Dashed lines indicate changes in the GRT (31.5, 63 and 18 s). Solid lines represent the strategies set for the electron acceptor (Automatic NO_3^- injection, 1% O_2 supply and NO_3^- injection stoppage).

372

373 3.2.4 Strategies related to the final electron acceptor

374 After the assessment of the GRT in Stages I, II and III-a, the operation of the HF-MBR in the next
 375 stages were devoted to evaluate different strategies to enhance the performance and the stability
 376 of the system. Up until day 73, the nitrate input was only provided by the periodic replacement of
 377 the mineral medium solution. Thus, the NO_3^- concentration available for the biomass was highly
 378 fluctuant, as depicted in Fig. 7B. In order to avoid such fluctuation, at day 74, an automatic
 379 injection of a NO_3^- solution was started by means of a syringe pump. The concentration of NO_3^-
 380 was then maintained between 1.7 and 2.2 g L^{-1} , based on literature (Muñoz *et al.*, 2013).
 381 Moreover, the recycling solution replacement was decreased to a dilution rate of 0.1 d^{-1} to avoid
 382 so frequent washings of the biomass suspended in the recycling solution. Resulting from this
 383 strategy, a NO_3^- consume of roughly 50 mg (L d)^{-1} (Fig. 7B) supported an efficient removal of the
 384 VOCs and a less oscillating removal of siloxanes.

385 In stage IV (days 101-152) the GRT was decreased back to 18 s in order to evaluate the influence
386 of the strategies over the removal of all the target pollutants, given the fact that toluene and
387 limonene were already removed due to higher GRTs. A sudden decrease in the performance of
388 the HF-MBR occurred at day 104 due to membrane clogging. This clogging was attributed to the
389 long operation time rather than the change in the EBRT. Its effect was most remarkably observed
390 for both toluene and limonene, whose REs dropped to 24 and 30%, respectively. The membrane
391 cleaning at day 108 allowed for the recovery of both target pollutants removal, which increased
392 to average REs of 83 ± 12 and $94 \pm 5\%$, clearly higher than those recorded in the first period that
393 operated at the same GRT. Hexane removal was also achieved higher than in the first period, its
394 RE increased from 5 to 21%. The performance of the HF-MBR towards siloxanes was more stable
395 within this period with ECs of 1.7 ± 0.2 and $3.9 \pm 0.7 \text{ g m}^{-3} \text{ h}^{-1}$. The concentration of electron
396 acceptor decreased after reducing the GRT to 18 s, so the NO_3^- injection had to be adjusted due
397 to an incremented consume of ca. 80 mg (L d)^{-1} .

398 3.2.5 Oxygen contribution

399 Considering that the common content of oxygen in biogas (Rasi *et al.*, 2007) is ca. 1%, the
400 following strategy adopted regarding the final electron acceptor was implemented at day 133
401 (days 134-152) and consisted in supplementing the gas matrix with a 1% of O_2 . The RE of hexane
402 stabilized at $14 \pm 5\%$, slightly higher compared to the operation with NO_3^- alone. An enhanced
403 RE was also observed for toluene, whose RE stabilized at $94 \pm 3\%$ and EC at $4.3 \pm 0.2 \text{ g m}^{-3} \text{ h}^{-1}$.
404 For the rest of pollutants, no significant difference was distinguished when O_2 was incorporated.
405 79 ± 4 , 15 ± 2 and $14 \pm 2\%$ steady state REs were recorded for limonene, D4 and D5 respectively,
406 corresponding to ECs of 30.5 ± 1.5 , 1.4 ± 0.2 and $2.6 \pm 0.7 \text{ g m}^{-3} \text{ h}^{-1}$.

407 The highest CO_2 production was recorded in this stage corresponding to an average $28 \pm 6 \text{ g C m}^{-3}$
408 h^{-1} (Fig. 7A). However, the pollutants removal accounted for $45 \pm 12 \text{ g C m}^{-3} \text{ h}^{-1}$, giving a rough
409 CME of 65 %, which was lower than in the previous stage. In this sense, a shorter residence time
410 implied lower RE and therefore an incomplete oxidation of limonene towards CO_2 , which was
411 also observed in stage I. The change in the residence time affected specially the removal of

412 limonene (Fig. 5C), and simultaneously the presence of α -terpinene was recorded, which
413 eventually decreased the CME (Fig. 7A).

414 At the light of the results, the automatic infusion of nitrate was stopped at day 152 for investigating
415 the capacity of the O_2 to act as sole electron acceptor. Limonene and toluene REs stabilized at 92
416 ± 1 and 98 ± 2 , respectively, which was higher than the REs obtained with NO_3^- alone. The RE
417 of hexane, D4 and D5 were maintained at similar values than those accomplished with nitrate. In
418 this sense, the input of a 1% of O_2 in the gas matrix supported an efficient performance of the HF-
419 MBR. These results suggest that the supplementation of NO_3^- to provide the microbial consortium
420 with electron acceptor would not be necessary, which would eventually reduce the operating costs
421 of the technology, because 1% is the common concentration of O_2 in typical biogas streams.

422

423 **4. CONCLUSIONS**

424 The present work confirmed the potential of PDMS membranes to separate siloxanes as well as
425 other biogas impurities such as toluene and limonene from synthetic biogas gas towards a clean
426 air stream. The presence of water in the other side of the membrane hindered the permeability of
427 hexane, D4 and D5 due to their hydrophobic nature. The biofilm grown in the shell side of a HF-
428 MBR enabled a complete transference of toluene and limonene when the gas residence time was
429 above 31.5 s, and also a higher diffusion of hexane. The quantification of the CO_2 in the outlet of
430 the HF-MBR confirmed the degradation of the pollutants and high carbon mineralization
431 efficiencies were obtained reaching values above 90%.

432 Several strategies regarding the final electron acceptor were performed. Supplementing the gas
433 with a 1% of O_2 supported an efficient performance of the bioreactor, which eventually would
434 reduce the costs of the technology since it is the common oxygen content in biogas.

435

436 **Funding:** This work was funded by the Spanish Ministry of Science, Innovation and Universities
437 (CTQ2014-53718-R) co-funded by FEDER and University of Girona. Eric Santos-Clotas thanks

438 Universitat de Girona for his predoctoral grant (IFUdG-2015/51). Alba Cabrera-Codony
439 acknowledges support from the European Union's Horizon 2020 research and innovation
440 programme under the Marie Skłodowska-Curie grant agreement N° 712949 (TECNIOspring
441 PLUS) and from the Agency for Business Competitiveness of the Government of Catalonia
442 (TECSPR16-1-0045). LEQUIA has been recognized as consolidated research groups by the
443 Catalan Government (2017-SGR-1552 and 2017SGR-548, respectively).

444 **Declaration of interests:** The authors declare no conflict of interests.

445

446 5. REFERENCES

- 447 1. (APHA), A.P.H.A., 1998. Standard Methods for the Examination of Water and Wastewater,
448 20th ed. Washington, USA.
- 449 Accettola, F., Guebitz, G.M., Schoeftner, R., 2008. Siloxane removal from biogas by
450 biofiltration: Biodegradation studies. *Clean Technol. Environ. Policy* 10, 211–218.
451 <https://doi.org/10.1007/s10098-007-0141-4>
- 452 Ajhar, M., Bannwarth, S., Stollenwerk, K.H., Spalding, G., Yüce, S., Wessling, M., Melin, T.,
453 2012. Siloxane removal using silicone-rubber membranes. *Sep. Purif. Technol.* 89, 234–
454 244. <https://doi.org/10.1016/j.seppur.2012.01.003>
- 455 Bak, C. u., Lim, C.J., Lee, J.G., Kim, Y.D., Kim, W.S., 2019. Removal of sulfur compounds
456 and siloxanes by physical and chemical sorption. *Sep. Purif. Technol.* 209, 542–549.
457 <https://doi.org/10.1016/j.seppur.2018.07.080>
- 458 Barbusinski, K., Kalemba, K., Kasperczyk, D., Urbaniec, K., Kozik, V., 2017. Biological
459 methods for odor treatment e A review costs Thermal oxidation Catalytic oxidation
460 Chemical scrubbing Adsorption Bioscrubbing Chemical neutralisation Biofiltration. *J.*
461 *Clean. Prod.* 152, 223–241. <https://doi.org/10.1016/j.jclepro.2017.03.093>
- 462 Boada, E., Santos-Clotas, E., Bertran, S., Cabrera-Codony, A., Gich, F., Martín, M.J., Ba, L.,
463 2020. Potential use of *Methylibium* sp. as a biodegradation tool in organosilicon and
464 volatile compounds removal for biogas upgrading 240.
465 <https://doi.org/10.1016/j.chemosphere.2019.124908>
- 466 Cabrera-Codony, A., Georgi, A., Gonzalez-Olmos, R., Valdés, H., Martín, M.J., 2017. Zeolites
467 as recyclable adsorbents/catalysts for biogas upgrading: Removal of
468 octamethylcyclotetrasiloxane. *Chem. Eng. J.* 307.
469 <https://doi.org/10.1016/j.cej.2016.09.017>
- 470 Cabrera-Codony, A., Gonzalez-Olmos, R., Martín, M.J., 2015. Regeneration of siloxane-
471 exhausted activated carbon by advanced oxidation processes. *J. Hazard. Mater.* 285, 501–
472 8. <https://doi.org/10.1016/j.jhazmat.2014.11.053>
- 473 Cabrera-Codony, A., Montes-Morán, M.A., Sánchez-Polo, M., Martín, M.J., Gonzalez-Olmos,
474 R., 2014. Biogas upgrading: Optimal activated carbon properties for siloxane removal.
475 *Environ. Sci. Technol.* 48. <https://doi.org/10.1021/es501274a>
- 476 Cabrera-Codony, A., Santos-Clotas, E., Ania, C.O., Martín, M.J., 2018. Competitive siloxane
477 adsorption in multicomponent gas streams for biogas upgrading. *Chem. Eng. J.* 344.

478 <https://doi.org/10.1016/j.cej.2018.03.131>

479 de Arespacochaga, N., Valderrama, C., Raich-Montiu, J., Crest, M., Mehta, S., Cortina, J.L.,
480 2015. Understanding the effects of the origin, occurrence, monitoring, control, fate and
481 removal of siloxanes on the energetic valorization of sewage biogas—A review. *Renew.*
482 *Sustain. Energy Rev.* 52, 366–381. <https://doi.org/10.1016/j.rser.2015.07.106>

483 Dewil, R., Appels, L., Baeyens, J., 2006. Energy use of biogas hampered by the presence of
484 siloxanes. *Energy Convers. Manag.* 47, 1711–1722.
485 <https://doi.org/10.1016/j.enconman.2005.10.016>

486 Kumar, A., Dewulf, J., Luvsanjamba, M., Van Langenhove, H., 2008a. Continuous operation of
487 membrane bioreactor treating toluene vapors by *Burkholderia vietnamiensis* G4. *Chem.*
488 *Eng. J.* <https://doi.org/10.1016/j.cej.2007.09.039>

489 Kumar, A., Dewulf, J., Van Langenhove, H., 2008b. Membrane-based biological waste gas
490 treatment. *Chem. Eng. J.* 136, 82–91. <https://doi.org/10.1016/j.cej.2007.06.006>

491 Lebrero, R., Gondim, A.C., Pérez, R., García-Encina, P.A., Muñoz, R., 2014. Comparative
492 assessment of a biofilter, a biotrickling filter and a hollow fiber membrane bioreactor for
493 odor treatment in wastewater treatment plants. *Water Res.* 49, 339–350.
494 <https://doi.org/10.1016/j.watres.2013.09.055>

495 Lebrero, R., Rodríguez, E., Estrada, J.M., García-Encina, P.A., Muñoz, R., 2012. Odor
496 abatement in biotrickling filters: Effect of the EBRT on methyl mercaptan and
497 hydrophobic VOCs removal. *Bioresour. Technol.* 109, 38–45.
498 <https://doi.org/10.1016/j.biortech.2012.01.052>

499 Lebrero, R., Volckaert, D., Pérez, R., Muñoz, R., Van Langenhove, H., 2013. A membrane
500 bioreactor for the simultaneous treatment of acetone, toluene, limonene and hexane at
501 trace level concentrations. *Water Res.* 47, 2199–2212.
502 <https://doi.org/10.1016/j.watres.2013.01.041>

503 Montebello, A.M., Mora, M., López, L.R., Bezerra, T., Gamisans, X., Lafuente, J., Baeza, M.,
504 Gabriel, D., 2014. Aerobic desulfurization of biogas by acidic biotrickling filtration in a
505 randomly packed reactor. *J. Hazard. Mater.* 280, 200–208.
506 <https://doi.org/10.1016/j.jhazmat.2014.07.075>

507 Mudliar, S., Giri, B., Padoley, K., Satpute, D., Dixit, R., Bhatt, P., Pandey, R., Juwarkar, A.,
508 Vaidya, A., 2010. Bioreactors for treatment of VOCs and odours - A review. *J. Environ.*
509 *Manage.* <https://doi.org/10.1016/j.jenvman.2010.01.006>

510 Muñoz, R., Meier, L., Diaz, I., Jeison, D., 2015. A review on the state-of-the-art of
511 physical/chemical and biological technologies for biogas upgrading. *Rev. Environ. Sci.*
512 *Biotechnol.* 14, 727–759. <https://doi.org/10.1007/s11157-015-9379-1>

513 Muñoz, R., Souza, T.S.O., Glittmann, L., Pérez, R., Quijano, G., 2013. Biological anoxic
514 treatment of O₂-free VOC emissions from the petrochemical industry: A proof of concept
515 study. *J. Hazard. Mater.* 260, 442–450. <https://doi.org/10.1016/j.jhazmat.2013.05.051>

516 Papadias, D., Ahmed, S., Kumar, R., 2011. Fuel Quality Issues in Stationary Fuel Cell Systems.

517 Papurello, D., Silvestri, S., Lanzini, A., 2019. Biogas cleaning: Trace compounds removal with
518 model validation. *Sep. Purif. Technol.* 210, 80–92.
519 <https://doi.org/10.1016/j.seppur.2018.07.081>

520 Pokorna-Krayzelova, L., Bartacek, J., Vejmelkova, D., Alvarez, A.A., Slukova, P., Prochazka,
521 J., Volcke, E.I.P., Jenicek, P., 2017. The use of a silicone-based biomembrane for
522 microaerobic H₂S removal from biogas. *Sep. Purif. Technol.* 189, 145–152.
523 <https://doi.org/10.1016/j.seppur.2017.07.077>

524 Popat, S.C., Deshusses, M. a., 2008. Biological removal of siloxanes from landfill and digester
525 gases: Opportunities and challenges. *Environ. Sci. Technol.* 42, 8510–8515.

526 <https://doi.org/10.1021/es801320w>

527 Rasi, S., Veijanen, A., Rintala, J., 2007. Trace compounds of biogas from different biogas
528 production plants. *Energy* 32, 1375–1380. <https://doi.org/10.1016/j.energy.2006.10.018>

529 Reij, M.W., Keurentjes, J.T.F., Hartmans, S., 1998. Membrane bioreactors for waste gas
530 treatment. *J. Biotechnol.* 59, 155–167.

531 Santos-Clotas, E., Cabrera-Codony, A., Boada, E., Gich, F., Muñoz, R., Martín, M.J., 2019a.
532 Efficient removal of siloxanes and volatile organic compounds from sewage biogas by an
533 anoxic biotrickling filter supplemented with activated carbon. *Bioresour. Technol.* 294,
534 122136. <https://doi.org/10.1016/j.biortech.2019.122136>

535 Santos-Clotas, E., Cabrera-Codony, A., Castillo, A., Martín, M.J., Poch, M., Monclús, H.,
536 2019b. Environmental Decision Support System for Biogas Upgrading to Feasible Fuel.
537 *Energies* 12, 1546. <https://doi.org/10.3390/en12081546>

538 Schweigkofler, M., Niessner, R., 2001. Removal of siloxanes in biogases 83, 183–196.

539 Soreanu, G., Béland, M., Falletta, P., Edmonson, K., Svoboda, L., Al-Jamal, M., Seto, P., 2011.
540 Approaches concerning siloxane removal from biogas - A review. *Can. Biosyst. Eng. / Le*
541 *Genie des Biosyst. au Canada* 53.

542 Wang, J., Zhang, W., Xu, J., Li, Y., Xu, X., 2014. Octamethylcyclotetrasiloxane removal using
543 an isolated bacterial strain in the biotrickling filter. *Biochem. Eng. J.* 91, 46–52.
544 <https://doi.org/10.1016/j.bej.2014.07.003>

545 Wheless, E., Pierce, J., 2004. Siloxanes in landfill and digester gas update. *SCS Eng. Environ.*
546 *Consult. Contract.* 1–10.

547 Zhang, Z., Qi, H., Ren, N., Li, Y., Gao, D., Kannan, K., 2011. Survey of cyclic and linear
548 siloxanes in sediment from the Songhua River and in sewage sludge from wastewater
549 treatment plants, Northeastern China. *Arch. Environ. Contam. Toxicol.* 60, 204–211.
550 <https://doi.org/10.1007/s00244-010-9619-x>

551 Zhao, K., Xiu, G., Xu, L., Zhang, D., Zhang, X., Deshusses, M.A., 2011. Biological treatment
552 of mixtures of toluene and n-hexane vapours in a hollow fibre membrane bioreactor
553 Biological treatment of mixtures of toluene and n-hexane vapours in a hollow fibre
554 membrane bioreactor. *Environ. Technol.* 32, 617–623.
555 <https://doi.org/10.1080/09593330.2010.507634>

556

557

558

559